Hemizygous Disruption of *Cdc25A* Inhibits Cellular Transformation and Mammary Tumorigenesis in Mice

Dipankar Ray,[1] Yasuhisa Terao,[3] Dipali Nimbalkar,[1] Hiroyuki Hirai,[1] Evan C. Osmundson,[1,3] Xianghong Zou,[3] Roberta Franks,[4] Konstantin Christov,[5] and Hiroaki Kiyokawa[1,2,3]

[1]Department of Molecular Pharmacology and Biological Chemistry and [2]Robert H. Lurie Comprehensive Cancer Center, Northwestern University, and [3]Department of Biochemistry and Molecular Genetics, [4]Research Resources Center, and [5]Department of Surgical Oncology, University of Illinois College of Medicine, Chicago, Illinois

Abstract

CDC25A phosphatase activates multiple cyclin-dependent kinases (CDK) during cell cycle progression. Inactivation of CDC25A by ubiquitin-mediated degradation is a major mechanism of DNA damage-induced S-G_2 checkpoint. Although increased CDC25A expression has been reported in various human cancer tissues, it remains unclear whether CDC25A activation is a critical rate-limiting step of carcinogenesis. To assess the role for CDC25A in cell cycle control and carcinogenesis, we used a *Cdc25A*-null mouse strain we recently generated. Whereas *Cdc25A*$^{-/-}$ mice exhibit early embryonic lethality, *Cdc25A*$^{+/-}$ mice show no appreciable developmental defect. *Cdc25A*$^{+/-}$ mouse embryonic fibroblasts (MEF) exhibit normal kinetics of cell cycle progression at early passages, modestly enhanced G_2 checkpoint response to DNA damage, and shortened proliferative life span, compared with wild-type MEFs. Importantly, *Cdc25A*$^{+/-}$ MEFs are significantly resistant to malignant transformation induced by coexpression of *H-ras*^{V12} and a dominant negative p53 mutant. The rate-limiting role for CDC25A in transformation is further supported by decreased transformation efficiency in MCF-10A human mammary epithelial cells stably expressing CDC25A small interfering RNA. Consistently, *Cdc25A*$^{+/-}$ mice show substantially prolonged latency in mammary tumorigenesis induced by MMTV-*H-ras* or MMTV-*neu* transgene, whereas MMTV-*myc*–induced tumorigenesis is not significantly affected by *Cdc25A* heterozygosity. Mammary tissues of *Cdc25A*$^{+/-}$;MMTV-*neu* mice before tumor development display less proliferative response to the oncogene with increased tyrosine phosphorylation of CDK1/2, but show no significant change in apoptosis. These results suggest that *Cdc25A* plays a rate-limiting role in transformation and tumor initiation mediated by *ras* activation. [Cancer Res 2007;67(14):6605–11]

Introduction

Cyclin-dependent kinases (CDK) play central roles in promoting progression of the cell cycle in all eukaryotic cells (1). CDK activity undergoes multiple layers of regulatory processes, including association with cyclins and inhibitors and post-translational modifications of CDK proteins, such as phosphorylation and dephosphorylation. Although phosphorylation of the T loop, e.g., Thr^{161} of CDK1, is required for full activation of CDKs, phosphorylation around the ATP binding site, e.g., Tyr^{15} of CDK1, is inhibitory on the CDK activity. The inhibitory phosphorylation of CDKs is mediated by Wee1 or Myt1 kinases, and dephosphorylation of the sites is catalyzed by CDC25 family phosphatases (2). This inhibitory phosphorylation plays important roles in controlling the timing of CDK activation. CDK2 activated by association with cyclin E and cyclin A governs initiation and completion of DNA replication. CDC25A-mediated dephosphorylation of CDK2 is critical for appropriate progression of S phase. CDK1 activated by cyclin A and cyclin B plays an essential role in initiation and completion of mitosis. All CDC25 phosphatases, i.e., CDC25A, CDC25B, and CDC25C, are likely to collaborate in timely activation of CDK1-cyclin A and CDK1-cyclin B during G_2-M transition. However, cells with compound disruption of CDC25B and CDC25C display minimum change in cell cycle progression (3). In contrast, CDC25A may play a nonredundant role in CDK1 activation (4). Knockdown of CDC25A by RNA interference delays both G_1-S and G_2-M transitions (5), whereas overexpression of CDC25A can induce aberrant mitotic events (6).

Inactivation of CDC25 phosphatases is a major mechanism of cell cycle checkpoint (2). In response to DNA damage, activated CHK1 and CHK2 phosphorylate CDC25A and CDC25C (7, 8). It has been shown that CHK2-mediated phosphorylation inactivates CDC25C by cytoplasmic sequestration (7). On the other hand, CHK1-mediated CDC25A phosphorylation results in ubiquitination by the Skp1-Cullin-β-TrCP E3 complex and rapid proteasome-dependent degradation (9, 10). The CHK1-mediated CDC25A degradation leads to cell cycle arrest in S or G_2 phase. This is an acute response to DNA damage without employing new transcription or translation, in contrast to p53-dependent checkpoint responses involving transcription of $p21^{Cip1}$ (11) and 14-3-3σ (12, 13). CHK1 predominantly regulates cellular levels of CDC25A protein even during unperturbed cell cycle progression. Deregulation of checkpoint pathways is thought to play a key role in tumor progression. For instance, loss of the proximal checkpoint kinase ATM, which functions upstream of CHK1/2, strongly predisposes humans and mice to tumorigenesis (14, 15). Haploinsufficiency of another proximal kinase, ATR, promotes tumorigenesis in mice with defective DNA-mismatch repair (16). Furthermore, *Chk1* heterozygous mice exhibit enhanced tumorigenesis induced by Wnt-1 (17). Consistently with the notion that CDC25A is a major target of the Chk1 pathway, cellular CDC25A levels are increased in *Chk1*-heterozygous mice (18). CDC25A expression is significantly increased in a variety of human cancers, including head and neck, liver, thyroid, breast, ovary, and lung cancers (19–25). These observations suggest that tumor-suppressive

Note: Supplementary data for this article are available at Cancer Research Online (http://cancerres.aacrjournals.org/).

Current address for Y. Terao: Department of Obstetrics and Gynecology, Juntendo University, Tokyo 113-8421, Japan. Current address for X. Zou: Department of Pathology, Ohio State University, Columbus, OH 43221.

Requests for reprints: Hiroaki Kiyokawa, Department of Molecular Pharmacology & Biological Chemistry, Northwestern University, 303 E. Superior Street, Lurie 3-113, Chicago, IL 60611. Phone: 312-503-0699; Fax: 312-503-0700; E-mail: kiyokawa@northwestern.edu.

doi:10.1158/0008-5472.CAN-06-4815

action of the checkpoint pathway may depend largely on control of CDC25A expression within proper levels. In the present study, we examined whether CDC25A is rate limiting for cellular transformation and *in vivo* tumorigenesis using a newly generated *Cdc25A*-null mouse line.

Materials and Methods

Generation of mouse lines. *Cdc25A* mutant mouse lines were generated by gene targeting in a 129/sv mouse embryonic stem (ES) cell line, GS-1, followed by injection into C57BL/6 mouse embryos at the blastocyst stage, as previously described (26). Chimeras were then crossbred with wild-type C57BL/6 mice to generate germ line heterozygous mutants. Two ES clones, 2G6 and 2E11, went germ line, and homozygotes from both clones exhibited similar embryonic lethal phenotype. Therefore, mice from 2G6 were further characterized for this study. MMTV-*H-ras*, MMTV-*neu*, and MMTV-*myc* mice were described previously (27, 28). Mice were maintained according to protocols approved by the Institutional Animal Care Committees at Northwestern University and University of Illinois according to the AAALAS regulation. The primers used for genotyping PCR are SW39, 5′-ATATTGCTGAAGAGCTTGGCGG-3′, HK507, 5′-CTTCTGTTACTGTGTGTAGGATTGTTG-3′; and HK521, 5′-CTTTCTAGTGATCGGATGGTATATGGA-3′. The annealing temperature used for the 35-cycle PCR reaction was 62°C. To detect tumorigenesis, each mouse was physically examined twice a week, and the date of detecting palpable tumors was recorded. Mice were sacrificed when diameters of primary tumors reached 2 cm. For immunohistochemical analysis of proliferating cells, mice were injected i.p. with bromodeoxyuridine (BrdUrd, 50 μg/g body weight) at 2 h before sacrifice.

Cell cultures. Mouse embryonic fibroblasts (MEF) were isolated from day 12.5 mouse embryos and cultured as previously described (29). To determine cumulative population doublings, MEFs were cultured according to a 3T3 protocol, inoculated at the density of 3×10^5 per 25-cm^2 area (60-mm dish), and subcultured every 3 days. The population doubling level during each passage was calculated according to the formula: log(final cell number/3×10^5)/log 2. MCF-10A cells were cultured in DMEM/F12 supplemented with 5% heat-inactivated horse serum, 10 μg/mL insulin, 0.5 μg/mL hydrocortisone, 20 ng/mL recombinant human epithelial growth factor, 2 mmol/L L-glutamine, and 100 μg/mL penicillin/streptomycin. The sequences of small interfering RNAs (siRNA) 1 and 3 for targeting human CDC25A mRNA were 5′-AGCAACCACUGGAGGUGAAG-3 (residues 179–198) and 5′-AACCUUGACAACCGAUGCA-3′ (residues 751–769), respectively. Recombinant lentiviruses for expression of the siRNAs as short hairpin loops were constructed using the BLOCK-iT Lentiviral RNAi Expression System (Invitrogen) according to the manufacturer's instructions. Infected cells were selected with 10 μg/mL blasticidin. Retrovirus transduction of H-ras^{V12} plus DNp53 and soft-agar colony formation assays were done as previously described (30). Cell cycle analysis for serum-stimulated MEFs was done as previously described (29).

Immunologic analyses. For immunoblotting and immunoprecipitation, cells on culture dishes were scraped into lysis buffer and then sonicated as described previously (29). Anti-CDC25A monoclonal antibody (clone Ab3) was obtained from Neomarkers. Anti-BrdUrd monoclonal antibody was purchased from DAKO Inc. Phosphospecific anti-CDK1/2 rabbit polyclonal antibody was obtained from Calbiochem. Anti-CDK1 and CDK2 antibodies were purchased from Santa Cruz Biotechnology, and monoclonal β-actin (AC-15) antibody was from Sigma. The terminal nucleotidyl transferase–mediated nick end labeling (TUNEL) *in situ* hybridization kit was purchased from Oncor. Percentages of apoptotic cells and S-phase cells were determined by counting TUNEL- and BrdUrd-positive cells, respectively. Three animals per genotype were analyzed, and at least 600 epithelial cells per stained section were scored for quantification.

Checkpoint analysis. G_2 checkpoint was analyzed as described previously (5). Briefly, cells were mock irradiated or irradiated by 0.2–1.5 Gy IR from a ^{60}Co source. After 30 min incubation, cells were then treated with 100 ng/mL nocodazole to block mitotic progression of cells that did not arrest at G_2. Two hours later, cells were fixed and stained with propidium iodide and the phospho-histone H3 antibody (Upstate Biotechnology). Samples were then analyzed by flow-cytometric analyses using a Becton Dickinson FACScan, as described previously (31).

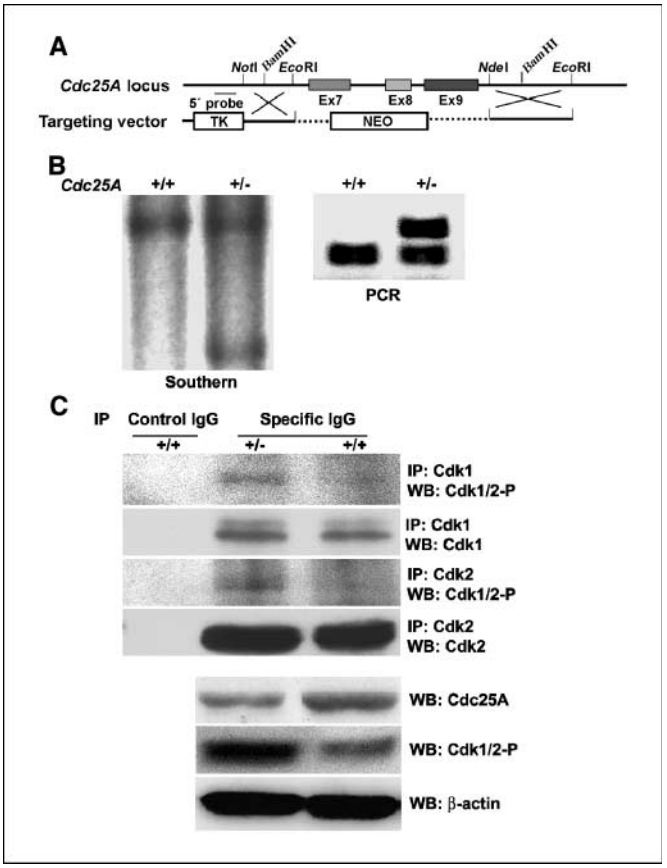

Figure 1. Heterozygous disruption of the *Cdc25A* gene results in decreased levels of CDC25A protein and increased tyrosine phosphorylation of CDK1 and CDK2. *A,* targeted disruption of murine *Cdc25A* gene. Targeting strategy for generation of *Cdc25A*-deficient mice is shown. *B,* Southern blotting and genomic PCR with tail DNA from a germ line heterozygous mutant and a wild-type littermate. *C,* CDC25A expression and tyrosine phosphorylation of CDK1/2 in *Cdc25A* heterozygous MEFs. *Bottom,* Western blots (*WB*) of MEF extracts using the indicated antibodies. *Top,* Western blots of immunoprecipitates (*IP*) with control nonspecific IgG or specific IgG from MEF extracts. *Cdk1/2-P,* an antibody specific for Tyr^{15} phosphorylation of CDK1/2.

Mammary gland whole mount. Inguinal mammary glands were dissected, spread onto glass slide, fixed in 10% buffered formalin, hydrated, stained overnight in 0.2% carmine (Sigma) and 0.5% $AlK(SO_4)_2$, dehydrated in graded solutions of ethanol, and cleared in Histoclear (National Diagnostics). Tissues were examined under an inverted microscope and photographed.

Statistical analyses. Kaplan-Meier tumor-free survival curves were compared between strains by the log-rank test analysis, and *P* values were determined. The significance did not change when the Wilcoxon test was used instead. Other statistical analyses were done using ANOVA and Student's *t* test.

Results

Hemizygous disruption of *Cdc25A* results in modestly enhanced G_2 checkpoint and shortened proliferative life span. To determine the roles of CDC25A in development and oncogenesis, we generated a *Cdc25A*-deficient mouse line by standard gene targeting in embryonic stem cells (Fig. 1*A* and *B*). Exons 7

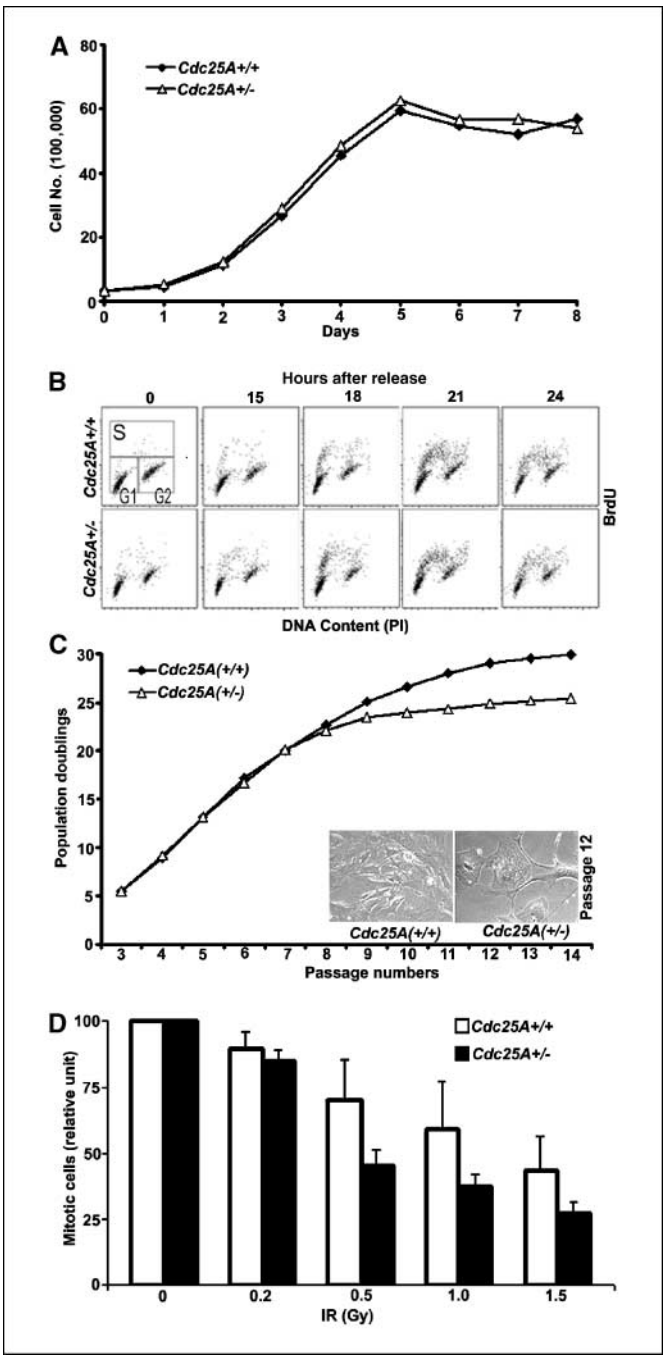

Figure 2. Cell cycle progression is minimally affected in *Cdc25A* heterozygous MEFs, whereas checkpoint response to DNA damage is modestly enhanced. *A,* growth curves of *Cdc25A*$^{+/-}$ and *Cdc25A*$^{+/+}$ MEFs (passage 3) prepared from the same litter. *B,* cell cycle progression of serum-deprived *Cdc25A*$^{+/-}$ and *Cdc25A*$^{+/+}$ MEFs after stimulation. Cells pulse-labeled with BrdUrd for 30 min were analyzed by flow cytometry after staining with propidium iodide and anti-BrdUrd antibody. *C,* shortened proliferative life span of *Cdc25A*$^{+/-}$ mouse embryonic fibroblasts. Cells with the indicated genotypes were cultured for continuous passages according to a 3T3 protocol (see Materials and Methods). Data representative of at least three independent cell preparations are shown. *Bottom inset,* Phase-microscopic pictures showing the morphology of MEFs at passage 12. *D,* enhanced G_2 checkpoint in *Cdc25A*$^{+/-}$ MEFs. MEFs were treated with ionizing irradiation (*IR*) at the indicated doses, followed by incubation at 30 min. Cells were then treated with nocodazole to block progression through metaphase. Two hours later, cells were fixed, stained with propidium iodide and anti-phospho-histone H3 antibody, and examined by flow cytometry. Percent decreases in mitotic populations of irradiated cultures, relative to nonirradiated controls, are shown as an indication of G_2 checkpoint function. *Columns,* means from three different cell preparations; *bars,* SE.

to 9 were replaced with a neomycin-resistant gene cassette. Intercross breeding of germ line heterozygous mice displayed that all homozygous mice died *in utero*. Histologic examinations of embryos revealed that homozygous mutants die at embryonic day 5 to 7 (E5-7), and homozygous blastocysts (E3.5 embryos) showed impaired hatching *in vitro*. This embryonic lethal phenotype of *Cdc25A*-null mice is being further characterized and will be reported elsewhere. *Cdc25A*-heterozygous (*Cdc25A*$^{+/-}$) mice seemed healthy and showed normal fertility and mammary function. For *ex vivo* studies, we prepared *Cdc25A*$^{+/-}$ and wild-type (*Cdc25A*$^{+/+}$) MEFs. Because of the early lethality, we were unable to isolate cells from *Cdc25A*$^{-/-}$ embryos. Immunoblotting showed that levels of CDC25A protein in *Cdc25A*$^{+/-}$ MEFs were about 40% lower than those in *Cdc25A*$^{+/+}$ MEFs (Fig. 1*C*). Immunoblotting with an antibody specific for CDK1/2 phosphorylated on Tyr^{15} showed that Tyr^{15} phosphorylation on these CDK proteins was increased by 1.6-fold in *Cdc25A*$^{+/-}$ MEFs. Immunoprecipitation of CDK1 or CDK2 followed by immunoblotting with the Tyr^{15} phosphospecific antibody further showed that tyrosine phosphorylation on both CDK1 and CDK2 was enhanced. These observations are consistent with the notion that CDC25A mediates tyrosine dephosphorylation of CDK1 and CDK2. *Cdc25A*$^{+/-}$ and *Cdc25A*$^{+/+}$ MEFs at early passages showed similar proliferation rates (Fig. 2*A*) despite the changes in CDC25A levels and CDK1/2 phosphorylation. *Cdc25A*$^{+/-}$ MEFs also exhibited normal kinetics of cell cycle entry from quiescence in response to serum stimulation (Fig. 2*B*, Supplementary Fig. S1). To further examine the replicative capacity of cells with hemizygous *Cdc25A* disruption, *Cdc25A*$^{+/-}$ and *Cdc25A*$^{+/+}$ MEFs were continuously cultured according to a 3T3 protocol (Fig. 2*C*). *Cdc25A*$^{+/-}$ and *Cdc25A*$^{+/+}$ MEFs exhibited comparable population doublings up to passage 8. *Cdc25A*$^{+/+}$ MEFs ceased proliferation by passages 14 to 16. *Cdc25A*$^{+/-}$ MEFs slowed down proliferation significantly earlier, displaying typical senescent morphology by passages 9 and 10. These observations suggest that hemizygous loss of *Cdc25A* shortens proliferative life span of primary fibroblasts. We then examined G_2 checkpoint response of *Cdc25A*$^{+/-}$ and *Cdc25A*$^{+/+}$ MEFs to DNA damage (Fig. 2*D*) using an experimental scheme previously applied for the characterization of *Cdc25B* and *Cdc25C* knock-out MEFs (5). MEFs were treated with increasing doses of ionizing irradiation (IR), and then the ability of G_2 cells to enter into mitosis within 2 h after IR was monitored. At 30 min after IR, nocodazole was added into culture media to block cells at the prometaphase. At 120 min after IR, percentages of mitotic cells were determined by flow cytometry. IR decreased progression of G_2 cells into mitosis, and the decrease was more remarkable in *Cdc25A*$^{+/-}$ cultures, relative to that in *Cdc25A*$^{+/+}$ cultures. Levels of CDC25B or CDC25C were not significantly different between *Cdc25A*$^{+/-}$ and *Cdc25A*$^{+/+}$ MEFs (data not shown). In contrast to the effect on G_2 checkpoint, *Cdc25A* heterozygosity minimally affected G_1 checkpoint, when *Cdc25A*$^{+/-}$ MEFs synchronized by serum starvation were treated with IR and restimulated with serum (Supplementary Fig. S2). No significant differences in DNA synthesis were observed in exponentially proliferating *Cdc25A*$^{+/-}$ and *Cdc25A*$^{+/+}$ MEFs exposed to IR, suggesting no major change in intra-S checkpoint (data not shown). These results suggest that *Cdc25A*$^{+/-}$ cells have modestly enhanced G_2 checkpoint and shortened proliferating life span, whereas unperturbed cell cycle progression during early passages is essentially unaltered.

Heterozygous disruption of CDC25A inhibits cellular transformation. To assess cellular potential to undergo transformation,

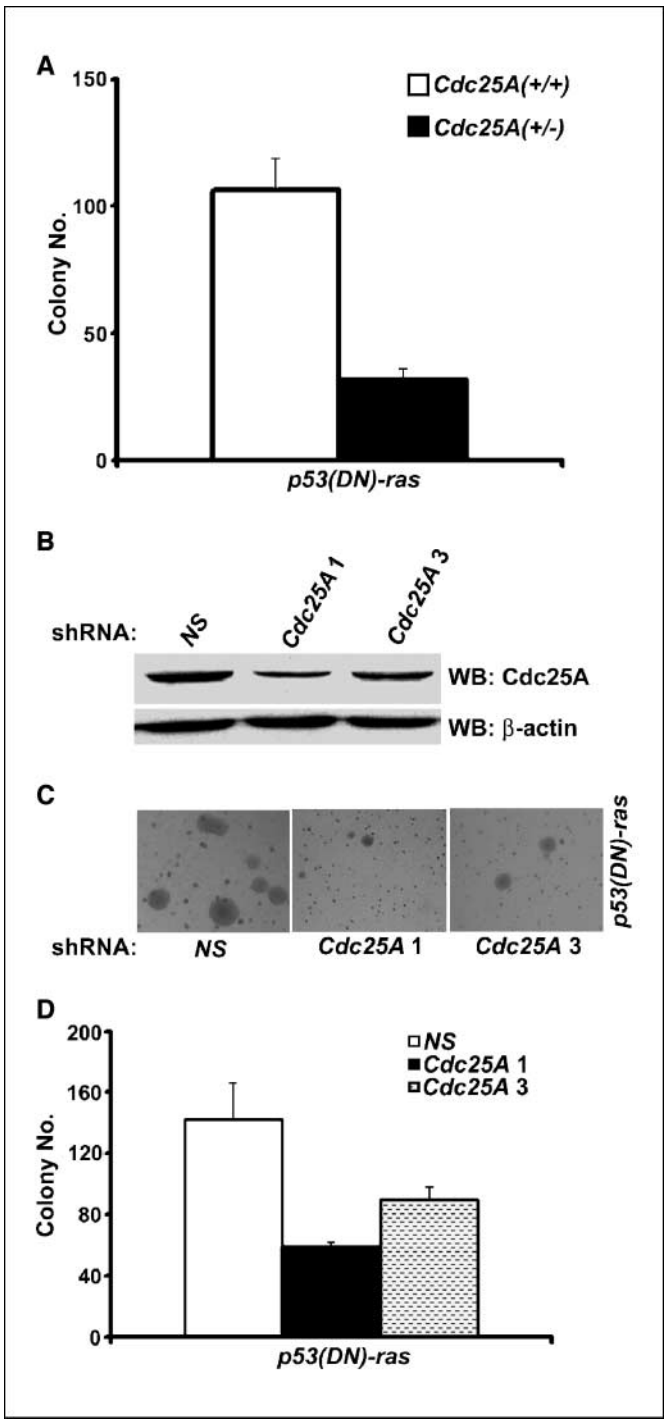

Figure 3. Cellular CDC25A levels play a rate-limiting role in *ras*-mediated transformation. *A,* transformation assays by scoring colony formation in soft agar following retroviral transduction of H-ras^{V12} and a dominant negative (*DN*) p53 mutant. Numbers of transformed colonies per plate scored on day 17 after plating are indicated as means + SE from three independent cell preparations per genotype. The difference is statistically significant ($P = 0.0086$). *B,* immunoblotting for CDC25A in human mammary epithelial MCF-10A cells expressing anti-CDC25A short hairpin RNA (shRNA 1 and 3) or control nonspecific (*NS*) double-stranded RNA. *C,* soft agar colony formation assay using MCF-10A cells with decreased CDC25A expression. Following the lentiviral shRNA transduction, cells were infected with retrovirus encoding H-ras^{V12} and a dominant negative p53 mutant. Cells were then plated in soft agar, and colony formation was scored. *D,* the numbers of colonies in soft agar per plate was scored on day 17 after plating and are shown as means + SE from three independent experiments. $P = 0.038$ and 0.069 for control versus Cdc25A shRNA 1 and 3, respectively.

Cdc25A$^{+/-}$ and *Cdc25A*$^{+/+}$ MEFs were infected with a bicistronic retrovirus encoding H-ras^{V12} and a dominant negative p53 mutant (DNp53; ref. 30) and then analyzed by colony formation in soft agar. *Cdc25A*$^{+/-}$ MEFs formed significantly fewer colonies in soft agar in response to the transforming stimuli, compared with *Cdc25A*$^{+/+}$ MEFs (Fig. 3*A*). Decreased susceptibility of *Cdc25A*$^{+/-}$ MEFs to transformation induced by H-ras^{V12} + DNp53 was also confirmed by focus formation assays in monolayer cultures (data not shown). These observations suggest that the cellular level of CDC25A is part of a rate-limiting mechanism of malignant transformation. To further delineate the role of CDC25A in transformation, we examined the effect of CDC25A knockdown in nontransformed human mammary epithelial MCF-10A cells. Two recombinant lentiviruses encoding different short hairpin RNAs, CDC25A shRNA 1 and 3, were used to knockdown CDC25A in MCF-10A cells. Lentiviral expression of shRNA 1 and 3 resulted in 57% and 35%

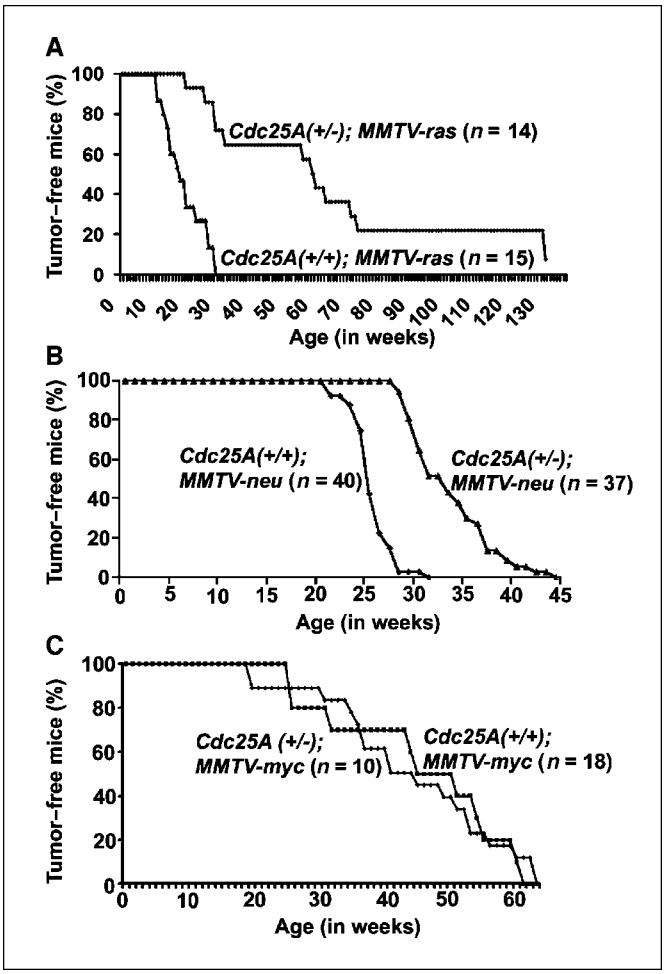

Figure 4. Delayed tumorigenesis of MMTV-*H-ras* and MMTV-*neu* mice in the *Cdc25A*$^{+/-}$ background. *A,* Kaplan-Meier tumor-free survival curves. The median time of tumor-free survival was 127 d for MMTV-*H-ras; Cdc25A*$^{+/+}$ mice and 419 d for MMTV-*H-ras*; *Cdc25A*$^{+/-}$ mice. Log-rank test analysis showed significant difference between the two groups ($P < 0.0001$). *B,* Kaplan-Meier survival curves. The median time of tumor-free survival was 180 d for MMTV-*neu*; *Cdc25A*$^{+/+}$ mice and 234 d for MMTV-*neu*; *Cdc25A*$^{+/-}$ mice. Log-rank test analysis showed significant difference between the two groups ($P < 0.0001$). *C,* Kaplan-Meier survival curves. The median time of tumor-free survival was 281 d for MMTV-*myc*; *Cdc25A*$^{+/+}$ mice and 312 d for MMTV-*myc*; *Cdc25A*$^{+/-}$ mice. The difference between the two groups was not statistically significant ($P = 0.510$).

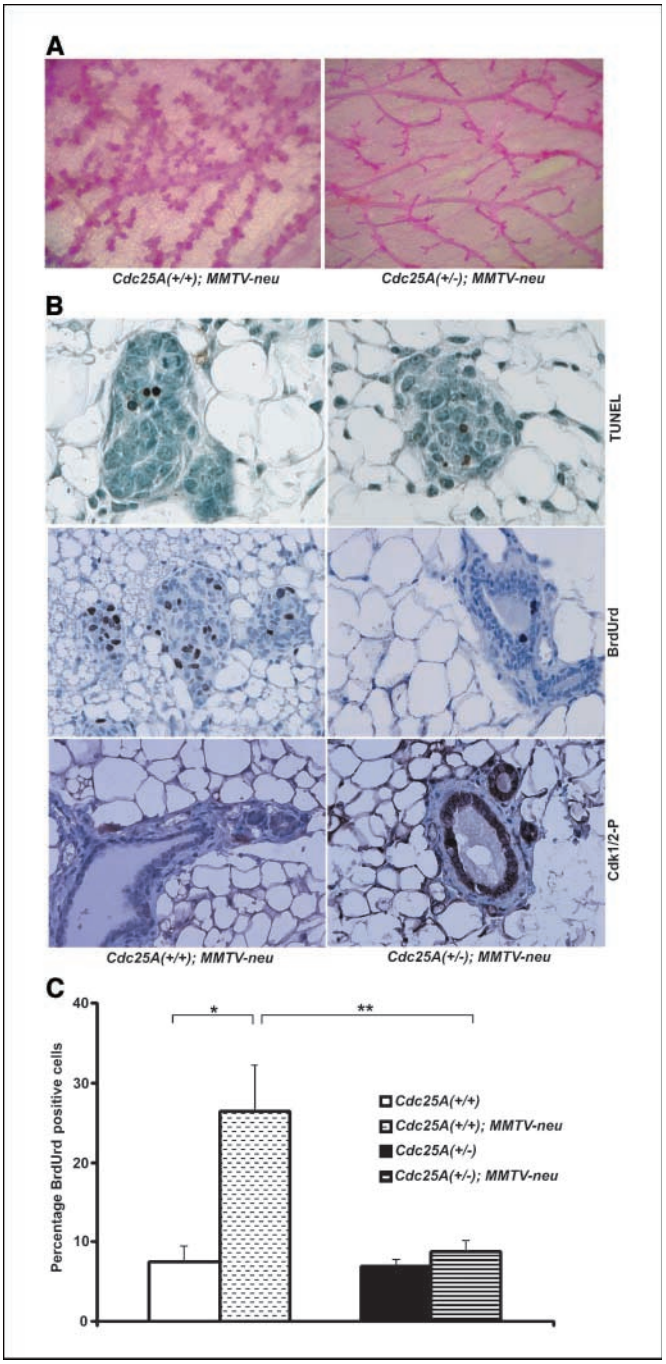

Figure 5. Mammary tissues of *Cdc25A*$^{+/-}$ mice expressing MMTV-*neu* oncogene display hypoproliferation with increased tyrosine phosphorylation of CDK proteins. *A,* whole-mount analysis of mammary glands from 12-wk-old mice with the indicated genotypes. *B,* TUNEL assay and immunohistologic analyses for BrdUrd incorporation and Tyr^{15} phosphorylation of CDK1/2 in mammary tissues of 5-wk-old mice. Mice with the indicated genotypes were administered i.p. with BrdUrd, and 2 h later, mammary tissues were sampled. *C,* the percentage of BrdUrd-positive cells in mammary epithelia of 5-week-old *Cdc25A*$^{+/+}$ and *Cdc25A*$^{+/-}$ mice in the presence and absence of *neu* oncogene are shown as a means + SE. *, $P = 0.008$; **, $P = 0.007$, statistically significant differences. The difference between *Cdc25A*$^{+/-}$ mice and *Cdc25A*$^{+/-}$; MMTV-*neu* mice was not statistically significant ($P = 0.315$).

decreases in cellular Cdc25A levels, respectively (Fig. 3*B*). These shRNAs did not significantly affect cellular levels of CDC25B or CDC25C and minimally affected the rate of proliferation (data not shown). To determine effects of CDC25A knockdown on transformation, at 24 h post-lentiviral infection, cells were infected with the H-ras^{V12} + DNp53 retrovirus. The expression of shRNA 1 and 3 decreased the numbers of transformed colonies by 58% and 36%, respectively, compared with control expression of nonspecific shRNA (Fig. 3*C* and *D*). When the shRNA lentiviruses were infected at 24 h after retroviral transduction of H-ras^{V12} + DNp53, we did not observe any significant difference in colony formation between the control and anti-CDC25A shRNAs (data not shown). These data suggest that cellular CDC25A levels at the time of oncogene activation are critical and indicate that CDC25A plays a rate-limiting role in *ras*-mediated transformation.

Hemizygous loss of *Cdc25A* delays *H-ras*- or *neu*-induced mammary tumorigenesis. *Cdc25A*$^{+/-}$ mice exhibited normal development of all examined tissues, including mammary glands (Supplementary Fig. S3). We then addressed the question whether *Cdc25A* heterozygosity inhibits *in vivo* tumorigenesis, by cross-breeding *Cdc25A*$^{+/-}$ mice with MMTV-*H-ras* or MMTV-*neu* transgenic mice, which are well-established models for spontaneous mammary tumorigenesis (27, 28). *Cdc25A*$^{+/+}$;MMTV-*H-ras* mice developed mammary and salivary tumors with average latency of 18 weeks (Fig. 4*A*). In striking contrast, the tumor latency of *Cdc25A*$^{+/-}$;MMTV-*H-ras* mice was 60 weeks, demonstrating a marked delay in tumorigenesis. It is noteworthy that about 10% of *Cdc25A*$^{+/-}$;MMTV-*H-Ras* mice did not develop detectable tumors over 2 years of monitoring. *Cdc25A*$^{+/-}$;MMTV-*neu* mice also exhibited significantly delayed tumorigenesis, with median latency of 32 weeks, relative to the latency of 23 weeks in *Cdc25A*$^{+/+}$;MMTV-*neu* mice (Fig. 4*B*). Thus, hemizygous loss of *Cdc25A* delays or inhibits *ras*- and *neu*-induced tumorigenesis. The macro- and microscopic morphologic characteristics and growth rates were indistinguishable between palpable (>0.5 cm) mammary adenocarcinomas induced by *H-ras* or *neu* in the *Cdc25A*$^{+/+}$ background and in *Cdc25A*$^{+/-}$ background (data not shown). To further characterize early events before tumor detection, we did whole-mount analyses of mammary tissues in virgin mice. Mammary glands from 12-week-old *Cdc25A*$^{+/+}$;MMTV-*neu* mice showed proliferative disturbances as evidenced by hyperplastic nodules (Fig. 5*A*), which is in concordance with previous reports (28). Mammary glands from *Cdc25A*$^{+/-}$;MMTV-*neu* mice exhibited grossly normal postnatal development of mammary epithelia, and focal proliferative lesions were less obvious. For a clue to the mechanism of the early changes rendered by *Cdc25A* heterozygosity, we then analyzed apoptosis and proliferation in mammary tissues from 5-week-old *Cdc25A*$^{+/-}$; MMTV-*neu* and *Cdc25A*$^{+/+}$;MMTV-*neu* mice (Fig. 5*B*). TUNEL analysis showed that there was no significant difference in apoptosis between the two groups. In contrast, percentages of S-phase cells, determined by BrdUrd immunohistochemistry, in mammary epithelia of *Cdc25A*$^{+/-}$;MMTV-*neu* mice were significantly lower than those of *Cdc25A*$^{+/+}$;MMTV-*neu* mice (8.65 $\pm$ 1.49% versus 26.4 $\pm$ 5.74%). Decreased proliferation in *Cdc25A*$^{+/-}$; MMTV-*neu* mammary epithelia was correlated with increased immunoreactivities to the antibody specific to Tyr^{15}-phosphorylated CDK1/2. These data suggest that hemizygous loss of CDC25A is inhibitory on tumor initiation, mostly by down-regulation of proliferation stimulated by the *neu-ras* oncogenic pathway. The cell proliferation in mammary epithelia was almost comparable between *Cdc25A*$^{+/+}$ and *Cdc25A*$^{+/-}$ mice without MMTV-*neu* (7.47 $\pm$ 1.99% versus 6.85 $\pm$ 1.49%; Fig. 5*C*, Supplementary Fig. S4). These data clearly suggest that the cellular level of Cdc25A is critical for oncogene-induced cell proliferation.

Finally, we examined the effect of *Cdc25A* heterozygosity on tumorigenesis initiated by another oncogenic signal, c-*myc* overexpression. *Cdc25A*$^{+/-}$ mice were crossbred with MMTV-*myc* transgenic mice, which is also a widely used murine mammary tumor model (27). In contrast to *ras*- and *neu*-induced tumorigenesis, the median tumor latency in *Cdc25A*$^{+/-}$;MMTV-*myc* mice was not statistically different from that in *Cdc25A*$^{+/+}$;MMTV-*myc* mice (44 weeks versus 40 weeks; Fig. 4*C*). Taken together, these *in vivo* effects of hemizygous CDC25A disruption suggest that cellular levels of CDC25A form a critical factor determining the efficacy of tumorigenesis initiated specifically by activation of the *neu-ras* oncogenic pathway.

Discussion

CDC25A activates multiple cyclin/CDK complexes throughout the cell cycle (5). The present study has shown that hemizygous disruption of the *Cdc25A* gene results in inhibition of *ras*-mediated transformation, although continuous cell cycle progression and serum-induced cell cycle entry are minimally affected. These observations suggest that the cellular level of CDC25A is rate limiting for malignant transformation that involves oncogenic action of *ras*. Consistently, tumorigenesis induced by the MMTV-*H-ras* or *neu* transgene is substantially delayed in *Cdc25A*$^{+/-}$ mice. The data showing that ~50% reduction in CDC25A expression is sufficient to inhibit tumor initiation indicate a critical role for CDC25A phosphatase in HER2/*neu-ras*–mediated mammary tumorigenesis. *Cdc25A* heterozygosity inhibits *ras*-induced tumorigenesis most remarkably and influences *neu*-induced tumorigenesis to a lesser extent. This difference implies that CDC25A activation is involved specifically in the *ras*–mitogen-activated protein kinase pathway, whereas other downstream targets of the Her2/*neu* oncogenic signal, e.g., the phosphoinositide-3-kinase-Akt pathway, may not depend on CDC25A. In contrast, *Cdc25A* heterozygosity had no significant effect on *myc*-induced tumorigenesis. These differential effects of the *Cdc25A*$^{+/-}$ background are reminiscent of those of cyclin D1 or Pin1 ablation. Both cyclin D1-null (*Ccnd1*$^{-/-}$) mice and Pin1-null (*Pin1*$^{-/-}$) mice are refractory to MMTV-*neu*- and MMTV-*H-ras*-induced tumorigenesis, whereas they are sensitive to MMTV-*myc*-induced tumorigenesis (32, 33). Pin1 seems to function upstream of cyclin D1 in mammary tumorigenesis (33). The detail of the interplay of CDC25A and cyclin D1 in the *neu-ras* oncogenic pathway is yet to be elucidated. The major substrates of CDC25A are thought to be CDK1 and CDK2, and it remains unclear whether CDC25A activates cyclin D-CDK4(CDK6) complex during normal cell cycle progression or oncogenic transformation. Because CDC25A is an E2F target gene (34), cyclin D1 overexpression may result in the up-regulation of CDC25A via E2F activation. The unaltered sensitivity of *Cdc25A*$^{+/-}$ mice to *myc*-induced tumorigenesis implies that CDC25A does not play a key role in the oncogenic action of *myc* despite a previous report that CDC25A is a *myc*-target gene (35). It is possible that like *Wnt-1, myc* overexpression may induce oncogenesis in stem cells or very early progenitor cells in the mammary tissue. On the other hand, activation of the *neu-ras* pathway might transform more differentiated mammary epithelial cells, depending on cyclin D1 and CDC25A activation. Further investigations are necessary to fully understand the specificity of oncogenic pathways that require CDC25A function.

The present study, as well as previous studies using knock-out mice, suggests diverse functions of the CDC25 family proteins. *Cdc25A*$^{-/-}$ mice are lethal during the peri-implantation period. *Cdc25A*$^{+/-}$ MEFs proliferate normally during early passages, but display modestly enhanced G_2 checkpoint response to DNA damage and markedly decreased efficiency in *ras*-mediated transformation. *Cdc25A*$^{+/-}$ MEFs also undergo senescence at earlier passages than wild-type MEFs do. Decreased sensitivity of *Cdc25A*$^{+/-}$ MEFs to transforming signals could be associated with premature senescence, according to the recent notion that senescence induced by oncogenic or oxidative stress is a potent barrier against malignant transformation (36). On the other hand, no substantial effects of *Cdc25A* heterozygosity on apoptosis were observed when MEFs were exposed to IR or serum starved (data not shown). Consistently, in mammary tissues of *Cdc25A*$^{+/-}$;MMTV-*neu* mice before tumor development, we observed decreased proliferation with increased Tyr^{15} phosphorylation, but no robust change in apoptosis. Thus, cells with reduced CDC25A expression seem to have impaired proliferative capacity in response to oncogenic stimuli or stress, whereas apoptotic responses seem to be unaltered. The inhibitory effect on proliferative capacity may account for the relative resistance of *Cdc25A*$^{+/-}$ mice to *neu/ras*-induced mammary tumorigenesis. Although CDC25A overexpression could affect apoptotic responses (37), the present study shows that hemizygous loss of CDC25A does not have major impacts on apoptotic control. In contrast with the phenotypes of *Cdc25A* knock-out mice, *Cdc25B*-null mice develop normally except for a meiotic defect during oogenesis (38). *Cdc25C*-null mice seem healthy (39). Interestingly, *Cdc25B*$^{-/-}$ MEFs and *Cdc25C*$^{-/-}$ MEFs exhibit no change in cell cycle progression or checkpoint function. Therefore, CDC25A plays a nonredundant role in embryogenesis and oncogenesis, whereas CDC25B and CDC25C are essentially dispensable. Although transgenic mice expressing CDC25B under the MMTV promoter display precocious alveolar hyperplasia (40) and modestly increased susceptibility to a carcinogen (41), it remains obscure whether CDC25B or CDC25C plays a rate-limiting role in oncogenesis. Taken together, among the CDC25 family, CDC25A is highlighted as an indispensable regulator of developmental and oncogenic proliferation.

Delayed tumorigenesis in the *Cdc25A*$^{+/-}$ background not only indicates the importance of CDC25A in tumor initiation, but also presents a scientific foundation for CDC25A as a potent therapeutic target. A clinical study reported that ~50% of $T_{1a,b}$ breast cancer tissues exhibited CDC25A overexpression, which correlated with poor survival (25). Our recent study showed that ectopic expression of CDC25A by an MMTV-*CDC25A* transgene significantly accelerates development of mammary tumors in MMTV-*H-ras* or MMTV-*neu* mice (42). Tumors with the MMTV-*CDC25A* transgene exhibit markedly accelerated growth and more invasive characteristics with chromosomal instability, which are consistent with the suggested role for CDC25A in malignant phenotypes of human breast cancer. Furthermore, the inhibitory effect of the *Cdc25a*$^{+/-}$ background on the *ras-neu* oncogenic pathway supports the rationale of using CDC25A inhibitors for therapeutic intervention. Multiple small-molecule agents including vitamin K analogues have been developed as pharmacologic inhibitors of CDC25 phosphatases (43–45). One of such CDC25 inhibitors, BN82685, exhibits *in vivo* tumor inhibitory activity as an orally bioactive agent (46). Further investigations are needed to establish chemotherapeutic strategies targeted on CDC25 phosphatases, especially for breast cancer with Her2/*neu* overexpression. The

mouse models with altered CDC25A levels will be useful tools for examining biological impacts of CDC25-targeted therapeutic intervention.

Acknowledgments

Received 12/31/2006; revised 4/19/2007; accepted 5/10/2007.

Grant support: H. Kiyokawa from the NIH (R01-CA100204, CA112282, and HD38085), the Department of Defense (DAMD 17-02-1-0413), the Searle Leadership Fund, the Zell Scholar Fund, and the Robert H. Lurie Comprehensive Cancer Center.

The costs of publication of this article were defrayed in part by the payment of page charges. This article must therefore be hereby marked *advertisement* in accordance with 18 U.S.C. Section 1734 solely to indicate this fact.

We thank Brian Zwecker, Suchitra Prasad, Alba Santana, Aileen Aziyu, Lida Aris, Kimberly Hansel, Shengben Liang, Anne Shilkaitis, Jadwiga Labanowska, the Transgenic Facility of the University of Illinois at Chicago, and the Center for Women's Health and Reproduction (U54 HD40093) for technical assistance and resources. We also thank Alfred Rademaker at the Biostatistics Core of Robert H. Lurie Comprehensive Cancer Center for statistical analyses, Hidayatullah Munshi, Nissim Hay, Navdeep Chandel, Vince Cryns, Thomas McGarry, Jill Pelling, Goberdhan Dimri, Puneet Opal, Siwanon Jirawatnotai, David Moons, and Mary Gillam for helpful suggestions and discussions.

References

1. Nurse P. A long twentieth century of the cell cycle and beyond. Cell 2000;100:71–8.
2. Donzelli M, Draetta GF. Regulating mammalian checkpoints through Cdc25 inactivation. EMBO Rep 2003;4:671–7.
3. Ferguson AM, White LS, Donovan PJ, Piwnica-Worms H. Normal cell cycle and checkpoint responses in mice and cells lacking Cdc25B and Cdc25C protein phosphatases. Mol Cell Biol 2005;25:2853–60.
4. Kallstrom H, Lindqvist A, Pospisil V, Lundgren A, Rosenthal CK. Cdc25A localisation and shuttling: characterisation of sequences mediating nuclear export and import. Exp Cell Res 2005;303:89–100.
5. Zhao H, Watkins JL, Piwnica-Worms H. Disruption of the checkpoint kinase 1/cell division cycle 25A pathway abrogates ionizing radiation-induced S and G_2 checkpoints. Proc Natl Acad Sci U S A 2002;99:14795–800.
6. Molinari M, Mercurio C, Dominguez J, Goubin F, Draetta GF. Human Cdc25 A inactivation in response to S phase inhibition and its role in preventing premature mitosis. EMBO Rep 2000;1:71–9.
7. Sanchez Y, Wong C, Thoma RS, et al. Conservation of the Chk1 checkpoint pathway in mammals: linkage of DNA damage to Cdk regulation through Cdc25. Science 1997;277:1497–501.
8. Mailand N, Falck J, Lukas C, et al. Rapid destruction of human Cdc25A in response to DNA damage. Science 2000;288:1425–9.
9. Busino L, Donzelli M, Chiesa M, et al. Degradation of Cdc25A by β-TrCP during S phase and in response to DNA damage. Nature 2003;426:87–91.
10. Jin J, Shirogane T, Xu L, et al. SCFβ-TRCP links Chk1 signaling to degradation of the Cdc25A protein phosphatase. Genes Dev 2003;17:3062–74.
11. el Deiry WS, Tokino T, Velculescu VE, et al. WAF1, a potential mediator of p53 tumor suppression. Cell 1993;75:817–25.
12. Bunz F, Dutriaux A, Lengauer C, et al. Requirement for p53 and p21 to sustain G_2 arrest after DNA damage. Science 1998;282:1497–501.
13. Chan TA, Hwang PM, Hermeking H, Kinzler KW, Vogelstein B. Cooperative effects of genes controlling the G(2)/M checkpoint. Genes Dev 2000;14:1584–8.
14. Savitsky K, Sfez S, Tagle DA, et al. The complete sequence of the coding region of the ATM gene reveals similarity to cell cycle regulators in different species. Hum Mol Genet 1995;4:2025–32.
15. Barlow C, Hirotsune S, Paylor R, et al. Atm-deficient mice: a paradigm of ataxia telangiectasia. Cell 1996;86:159–71.
16. Fang Y, Tsao CC, Goodman BK, et al. ATR functions as a gene dosage-dependent tumor suppressor on a mismatch repair-deficient background. EMBO J 2004;23:3164–74.
17. Liu Q, Guntuku S, Cui XS, et al. Chk1 is an essential kinase that is regulated by Atr and required for the G(2)/M DNA damage checkpoint. Genes Dev 2000;14:1448–59.
18. Lam MH, Liu Q, Elledge SJ, Rosen JM. Chk1 is haploinsufficient for multiple functions critical to tumor suppression. Cancer Cell 2004;6:45–59.
19. Gasparotto D, Maestro R, Piccinin S, et al. Overexpression of CDC25A and CDC25B in head and neck cancers. Cancer Res 1997;57:2366–8.
20. Xu X, Yamamoto H, Sakon M, et al. Overexpression of CDC25A phosphatase is associated with hypergrowth activity and poor prognosis of human hepatocellular carcinomas. Clin Cancer Res 2003;9:1764–72.
21. Ito Y, Yoshida H, Nakano K, et al. Expression of cdc25A and cdc25B proteins in thyroid neoplasms. Br J Cancer 2002;86:1909–13.
22. Broggini M, Buraggi G, Brenna A, et al. Cell cycle-related phosphatases CDC25A and B expression correlates with survival in ovarian cancer patients. Anticancer Res 2000;20:4835–40.
23. Wu W, Fan YH, Kemp BL, Walsh G, Mao L. Overexpression of cdc25A and cdc25B is frequent in primary non-small cell lung cancer but is not associated with overexpression of c-myc. Cancer Res 1998;58:4082–5.
24. Hernandez S, Hernandez L, Bea S, et al. cdc25 cell cycle-activating phosphatases and c-myc expression in human non-Hodgkin's lymphomas. Cancer Res 1998;58:1762–7.
25. Cangi MG, Cukor B, Soung P, et al. Role of the Cdc25A phosphatase in human breast cancer. J Clin Invest 2000;106:753–61.
26. Kiyokawa H, Kineman RD, Manova-Todorova KO, et al. Enhanced growth of mice lacking the cyclin-dependent kinase inhibitor function of p27(Kip1). Cell 1996;85:721–32.
27. Sinn E, Muller W, Pattengale P, Tepler I, Wallace R, Leder P. Coexpression of MMTV/v-Ha-ras and MMTV/c-myc genes in transgenic mice: synergistic action of oncogenes *in vivo*. Cell 1987;49:465–75.
28. Muller WJ, Sinn E, Pattengale PK, Wallace R, Leder P. Single-step induction of mammary adenocarcinoma in transgenic mice bearing the activated c-neu oncogene. Cell 1988;54:105–15.
29. Tsutsui T, Hesabi B, Moons DS, et al. Targeted disruption of CDK4 delays cell cycle entry with enhanced p27Kip1 activity. Mol Cell Biol 1999;19:7011–9.
30. Zou X, Ray D, Aziyu A, et al. Cdk4 disruption renders primary mouse cells resistant to oncogenic transformation, leading to Arf/p53-independent senescence. Genes Dev 2002;16:2923–34.
31. Xu B, Kim ST, Lim DS, Kastan MB. Two molecularly distinct G(2)/M checkpoints are induced by ionizing irradiation. Mol Cell Biol 2002;22:1049–59.
32. Yu Q, Geng Y, Sicinski P. Specific protection against breast cancers by cyclin D1 ablation. Nature 2001;411:1017–21.
33. Wulf G, Garg P, Liou YC, Iglehart D, Lu KP. Modeling breast cancer *in vivo* and *ex vivo* reveals an essential role of Pin1 in tumorigenesis. EMBO J 2004;23:3397–407.
34. Vigo E, Muller H, Prosperini E, et al. CDC25A phosphatase is a target of E2F and is required for efficient E2F-induced S phase. Mol Cell Biol 1999;19:6379–95.
35. Galaktionov K, Chen X, Beach D. Cdc25 cell-cycle phosphatase as a target of c-myc. Nature 1996;382:511–7.
36. Campisi J. Senescent cells, tumor suppression and organismal aging: good citizens, bad neighbors. Cell 2005;120:513–22.
37. Zou X, Tsutsui T, Ray D, Blomquist JF, Ichijo H, Ucker DS, Kiyokawa H. The cell cycle-regulatory CDC25A phosphatase inhibits apoptosis signal-regulating kinase 1. Mol Cell Biol 2001;21:4818–28.
38. Lincoln AJ, Wickramasinghe D, Stein P, et al. Cdc25b phosphatase is required for resumption of meiosis during oocyte maturation. Nat Genet 2002;30:446–9.
39. Chen MS, Hurov J, White LS, Woodford-Thomas T, Piwnica-Worms H. Absence of apparent phenotype in mice lacking Cdc25C protein phosphatase. Mol Cell Biol 2001;21:3853–61.
40. Ma ZQ, Chua SS, DeMayo FJ, Tsai SY. Induction of mammary gland hyperplasia in transgenic mice overexpressing human cdc25B. Oncogene 1999;18:4564–76.
41. Yao Y, Slosberg ED, Wang L, et al. Increased susceptibility to carcinogen-induced mammary tumors in MMTV-Cdc25B transgenic mice. Oncogene 1999;18:5159–66.
42. Ray D, Terao Y, Fuhrken PG, et al. Deregulated CDC25A expression promotes mammary tumorigenesis with genomic instability. Cancer Res 2007;67:284–91.
43. Kar S, Wang M, Ham SW, Carr BI. H32, a Non-Quinone Sulfone Analog of Vitamin K3, Inhibits Human Hepatoma Cell Growth by Inhibiting Cdc25 and Activating ERK. Cancer Biol Ther 2006;5:1340–7.
44. Kar S, Wang M, Yao W, Michejda CJ, Carr BI. PM-20, a novel inhibitor of Cdc25A, induces extracellular signal-regulated kinase 1/2 phosphorylation and inhibits hepatocellular carcinoma growth *in vitro* and *in vivo*. Mol Cancer Ther 2006;5:1511–9.
45. Contour-Galcera MO, Lavergne O, Brezak MC, Ducommun B, Prevost G. Synthesis of small molecule CDC25 phosphatases inhibitors. Bioorg Med Chem Lett 2004;14:5809–12.
46. Brezak MC, Quaranta M, Contour-Galcera MO, et al. Inhibition of human tumor cell growth *in vivo* by an orally bioavailable inhibitor of CDC25 phosphatases. Mol Cancer Ther 2005;4:1378–87.

Hemizygous Disruption of *Cdc25A* Inhibits Cellular Transformation and Mammary Tumorigenesis in Mice

Dipankar Ray, Yasuhisa Terao, Dipali Nimbalkar, et al.

Cancer Res 2007;67:6605-6611.